Int J Adv Manuf Technol (2013) 69:2041–2053
DOI 10.1007/s00170-013-5182-8

ORIGINAL ARTICLE

# A finishing cutter selection algorithm for additive/subtractive rapid pattern manufacturing

**Xiaoming Luo · Ye Li · Matthew C. Frank**

Received: 11 March 2013 / Accepted: 4 July 2013 / Published online: 23 July 2013


**Abstract** The additive/subtractive rapid pattern manufacturing (RPM) process sequentially deposits thick material slabs and then machines them into desired geometries in a layer-by-layer manner. Although most rapid manufacturing systems mainly intend to increase flexibility in manufacturing rather than to reduce processing speed, it is still practical to choose the optimized sets of cutters and machining parameters specifically for each layer to improve both the machining quality and efficiency. This paper presents an algorithm to automatically select finishing cutter geometry, diameter, and calculate machining parameters for the RPM process. Inputs to this algorithm are StereoLithography file from a computer-aided design model and a cutter library. Finishing cutter selection is based on geometry accessibility and machining process efficiency analysis. The algorithm has been implemented in RPM automatic process planning software and the experimental result on a sample part is presented to show the efficacy of this algorithm.

**Keywords** Rapid manufacturing · Accessibility · Cutter selection

## 1 Introduction

An additive/subtractive rapid pattern manufacturing (RPM) process was proposed by authors of this paper. The RPM process and its cutter selection problem are introduced first. Then, some previous cutter selection studies are reviewed.

X. Luo (✉) · M. C. Frank
Department of Industrial and Manufacturing Systems Engineering, Iowa State University, Ames, IA 50011, USA
e-mail: ming2008cn@gmail.com

Y. Li
Department of Industrial and Manufacturing Engineering and Technology, Bradley University, Peoria, IL 61625, USA

### 1.1 Rapid pattern manufacturing process

An RPM process creates a 3-D pattern by repeatedly stacking a thick material slab, cutting it to a certain layer thickness, and then machining the slab layer into desired geometry [1]. The RPM system uses three-axis single-sided milling operations with the assumption that the process is mainly suited for the creation of two-part patterns for molding and sand casting industry. The basic steps of this process are illustrated in Fig. 1.

Essentially, the RPM system is a branch of rapid manufacturing processes applied in pattern manufacturing, where one of the main advantages lies in automatic process planning [2]. The automated machining process flow in the RPM system is illustrated in Fig. 2. In each building cycle, a new material slab is deposited on the base or on the previously finished layer. Then the material slab is milled to the thickness calculated by a material deposition layer thickness algorithm [1]. A roughing operation removes most of the surplus material to quickly create the gross part geometry for each layer. Next, a finishing operation is used to more accurately machine surfaces and should ensure high-quality surfaces and dimensions. Optional semi-roughing operations may be applied between the roughing operation and finishing operation in order to further reduce the total machining time, since patterns usually have large dimensions.

Three-axis vertical computer numerical control (CNC) milling is the machining process that generates part geometry in RPM process. Raw materials used by RPM process are medium density fiberboard (MDF), wood, high-density foam, polyurethane, etc. As the first operation in RPM process, a face milling operation is used to cut the material slab to precalculated material deposition layer thickness. Among all machining operations involved in RPM process, face milling is the least dependent on part geometries.

Cutter diameter is a highly geometry related variable in milling operation. In RPM process, using cutters specific for

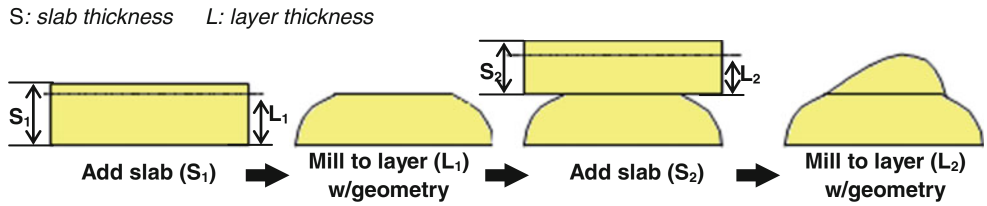


**Fig. 1** Illustration of RPM process

the geometry of each layer ensures good machining quality and saves machining time. Objectives of cutter selection are therefore to decide:

1. *Roughing cutter diameter and Stepdown.*
2. *Semi-roughing operations.*
3. *Finishing cutter geometry, diameter and Stepdown.*

This paper addresses the first part of cutter selection algorithm for RPM process, and it only discusses the finishing cutter geometry, diameter, and Stepdown selection.

Finishing operation uses surface finish contour cutter path. In surface finish contour milling, the cutter moves along contours or "waterlines" on part surfaces. As shown in Fig. 3, part surfaces are "simulated" with a group of contours. The finishing cutter follows these contours (cutter path) to "scan" all over along part surfaces until they are completely machined out. Stepdown is a parameter describing the distance along $z$ direction between two consecutive contours or "waterlines".

### 1.2 Literature review

As a highly skill-demanding task, cutter selection has been a major issue that hinders machining process planning from being automated. It is not easy to select cutters which are not only functionally correct but also optimum [3]. The development of software system for automatic cutter selection is still in its infancy [4]. Some early researches focused on finding the single best milling cutter for a particular feature [5, 6].

A geometric algorithm for finding the largest milling cutter for 2-D milling operations was presented by Yao et al. [7]. A feasible cutter definition based on cutter's ability to cover the target region was proposed. Even though the application of a single cutter selection was limited, it could be the first step for multiple cutter selection.

Bala et al. presented an automatic cutter selection and optimal cutter path generation method for prismatic parts [8]. Prismatic parts in their research were parts which were composed by prismatic features, such as slots, steps, projections, etc. Algorithms for selecting appropriate roughing and finishing cutters and generating the cutter path and NC code for machining a pocket were presented in their research. However, the single cutter for both roughing and finishing limited its application.

Chen et al. studied the optimal cutter selection and machining plane determination problem for die cavity roughing operation [9]. Both integer programming and dynamic programming were applied to search for the optimized cutter set and machining plane set to minimize the total machining time.

Other researchers addressed the problem of selecting multiple or a set of cutters for 2-D or 2½-D pocket machining. A 2½-D structure was composed of several 2-D planes, so they could be considered as the same type of problem. Arya et al. proposed an approximation algorithm to select multiple cutters from a set of cutters for milling a certain plane based on the minimum cost [10]. The running time and approximation ratio of this algorithm depended on the "simple cover complexity" of the milling region. A novel concept, Voronoi Mountain, was presented by Veeramani and Gau to calculate the material volume that could be removed by a specific cutter size [11, 12]. With the help of Voronoi Mountain, a dynamic programming model for selecting an optimal set of cutter sizes for 2½-D pocket machining on the basis of processing time was studied. Nadjakova and Mcmains also studied the problem of finding an optimal set of cutter for 2-D pocket machining on the basis of approximation ratio and machinable area [13]. Yao et al. expanded the cutter selection problem from the specific 2½-D feature to multiple parts milling field [14].

Wang et al. presented a computer-aided cutter selection system for 3-D die/mold-cavity NC machining using both a heuristic and analytical approach [15]. This approach selected cutter types, cutter sizes, and key parameters for dies and molds cavity machining.

D'Souza proposed a method to solve the cutter sequence selection for 2½-D pocket machining on setup level [16].

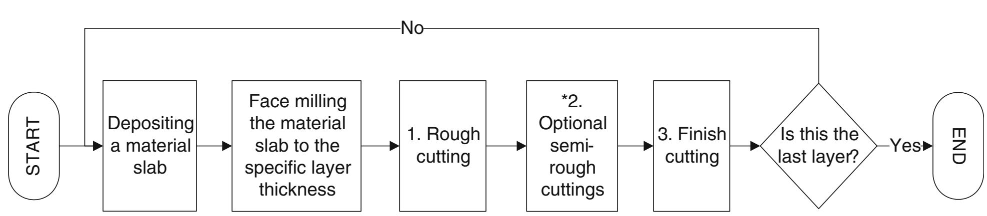


**Fig. 2** Flow chart of the automatic RPM process

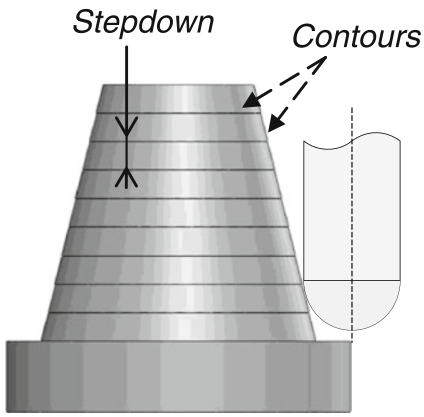


**Fig. 3** Finish contour cutter path

This method optimized the cutter path generation for all features in one setup, which might nest within each others from perspectives of: (a) feature level optimization, (b) composite cutter sequence graph optimization, (c) constrained graph optimization, and (d) subgraph optimization. A cost model based on the actual cutter path generation, including cutter path time, air path time, cutter change time, and cutter life time, was developed to evaluate solutions on cutter sequence selection. The complexity of the cutter sequence selection was reduced in their research by identifying the fact that "the accessible area of a larger cutter is a strict subset of the accessible area of a smaller cutter".

With feature-based models, precise geometry accessibility can be calculated and used for evaluating and selecting cutter sets. Lim et al. [17] developed an exact cutter sizing algorithm for feature accessibility. Cutter access distribution and relative delta-volume clearance data were created from cutter access algorithm, and adopted to select the optimum cutter automatically. The objective for cutter selection and cutter sizing in this algorithm was to study the geometric constraints imposed on cutter selection. The input to this algorithm was feature-based computer-aided design (CAD) models. The result from this algorithm was able to ensure good surface accessibility.

With the development of rapid prototyping and manufacturing, more and more attention is paid to cutter size selection for sculpture surface or free-form surface milling. Lee et al. [18] proposed a cut distribution and cutter selection method for sculpture surface cavity machining. A sculpture surface usually consists of free-form surface patches which were difficult and expensive to machine. Sculpture surface in this paper was defined by non-uniform rational B-spline surfaces which provided flexibility and freedom for surface description. Curvature evaluation was employed to select the finishing cutter. Roughing cutter size was based on cutters chosen for hunt planes in surface information evaluation and semi-roughing was based on geometric constraints and thickness of shoulders left on the surfaces. Cutter selection was optimized by the objective of high material remove rate (MRR). The difficulty in implementation of this system came from the determination of its system parameters.

Yang et al. [19] presented an interference detection and optimal cutter selection solution for three-axis NC machining of free-form surfaces. Three kinds of interference: protrusion interference, overlapping interference, and boundary collision interference were defined and relative solutions were proposed. The optimal cutter selection algorithm was based on the goal of minimum machining time. Objective surfaces in this paper were parametric surfaces. This method required high computational power when very fine grid resolution was used in these algorithms. Lin and Gian [20] proposed a multiple cutter approach to rough milling of sculpture surfaces depicted by ordered data points. In the beginning, cubic non-uniform B-spline surfaces were formed from the ordered data points and sliced with constant $z$ height to acquire the boundary and island loops in each layer. Then cutter sizes for linear pocketing, contour roughing, semi-roughing, and new-island processing operations were selected for good machining efficiency and cutter breakage prevention. Sun et al. [21] presented an algorithm for decomposing machining operations for free-form surface features in order to minimize machining time. Based on the decomposition of roughing and finishing, algorithms for roughing cutter and finishing cutter selection were also studied.

Many related researches in optimized cutter selection are based on MRR optimization [18, 19, 22]. MRR is mainly concerned with the machining efficiency. With the development of CAD/computer-aided manufacturing (CAM) technology, feature-based models have been widely adopted. Many feature-based algorithms have been developed since then [23, 24, 25]. By employing both the surface accessibility and MRR, feature-based algorithms lead to better precision in machining.

Determination on machining parameters was also studied by many research groups, for example in [26], [27], and [28]. Rad and Bidhendi [29] studied the optimum machining parameters determination problem for milling operations. Both single-cutter and multicutter operations were discussed in this research. A cutting force model based on two independent variables, 2-D chip-load and feed rate, were studied by Bae et al. [30]. An automatic feed rate adjustment method was proposed for optimal feed rate determination.

In summary, literatures reviewed above do not provide a systematic method for cutter geometry, cutter diameter, and machining parameters selection to support fully automatic machining process planning; moreover, none of them is based on layer-based machining. Therefore, this paper presents an algorithm to automatically select cutter geometry, cutter diameter, and Stepdown parameter for layers with different geometries in RPM process. The objective of this algorithm is to create the geometry of each layer maximally, and with better machining efficiency than that of existing fixed cutter set strategy.

## 2 Algorithm input data

There are two types of input data for the finishing cutter selection algorithm: geometry model and tool library. They are discussed in detail in this section.

### 2.1 Geometry model

Geometry input to this finishing cutter selection algorithm is StereoLithography (STL) file of a CAD model. STL model has become the de facto standard in rapid prototyping and manufacturing industry. It uses tessellated triangular facets to approximate part surfaces. Finishing cutter layer thicknesses are calculated based on STL model in this finishing cutter selection algorithm. Figure 4a illustrates an example of STL model.

In order to obtain part geometry at each $z$ axis position, an STL model is sliced along the $z$ axis to generate a set of 2-D polygonal cross-sections. These 2-D polygonal cross-sections are similar to contours or "waterlines" in finish contour cutter paths. Sliced STL model is used to calculate *accessibility ratio* (*AR*) of cutters in this algorithm. A sliced STL model is shown in Fig. 4b.

### 2.2 Cutter library

The machining process in RPM process is three-axis vertical CNC milling; therefore, cutters discussed here are milling cutters. The cutter library stores information of four cutter properties, which are cutter geometry (flat-end or sphere-end), cutter diameter (size), cutter speed, and Stepdown–feed relation.

Machining process efficiency is highly related to the cutter diameter. Cutters with larger diameter usually have high MRR. However, large diameter restricts the cutter's accessibility to small geometric features. In order to achieve optimal machining efficiency and geometric accessibility, a cutter library with a full range of cutter diameters is necessary, so that different cutters can be applied to different part geometries.

Flat and sphere ends are the most frequently used cutter geometries. Flat-end cutters have a planar end, which creates flat plane and large slope angle features with high efficiency. Sphere-end cutters are good at creating smooth curved surfaces with its half-sphere head. In the cutter library, there are always a flat-end cutter and a sphere-end cutter of the same diameter for selection.

Cutter speed, Stepdown, and feed rate are important parameters in machining process; and they are dependent on each other. In order to simplify the decision process of selecting these three parameters, cutter speeds are fixed in the first, based on cutter properties and machine characteristics.

Besides workpiece material property and cutter speed, the Stepdown and feed rate work together to affect the cutter load in machining. Each cutter has a safe cutting load. In machining operations, the feed rate has to reduce when Stepdown increases, and vice versa, in order to avoid overloading the cutter. In cutter library, a simple linear relation is used for Stepdown and feed rate calculation. As shown in Fig. 5, the Stepdown–feed linear relation is described with two end points [*Max Stepdown*, *Min Feed*] and [*Min Stepdown Max Feed*]. When either Stepdown or feed rate is known, the other one can be calculated according to this linear relation. For a specific cutter–material combination, two end points of the Stepdown–feed relation are stored in the cutter library. By the way, calculating the Stepdown–feed relation for each specific cutter–material combination is not the purpose of this paper and is not discussed here.

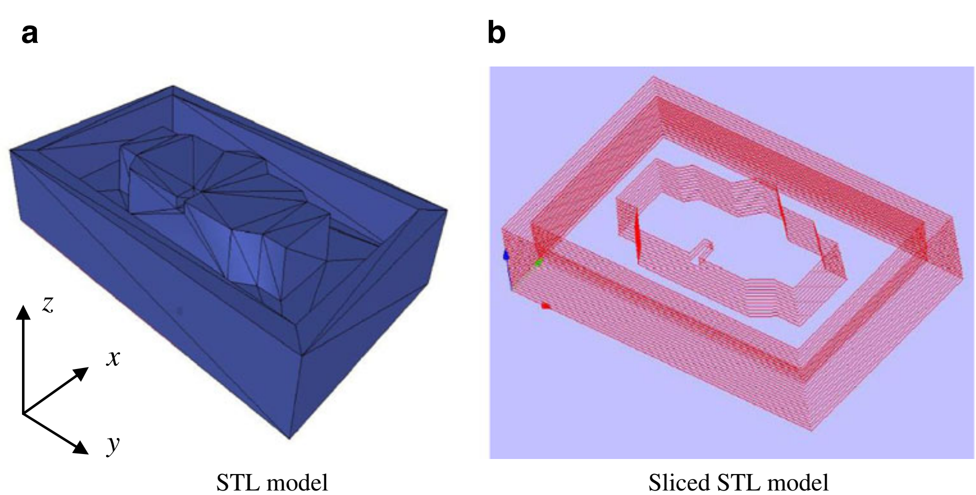


**Fig. 4** Examples of **a** STL model and **b** sliced STL model

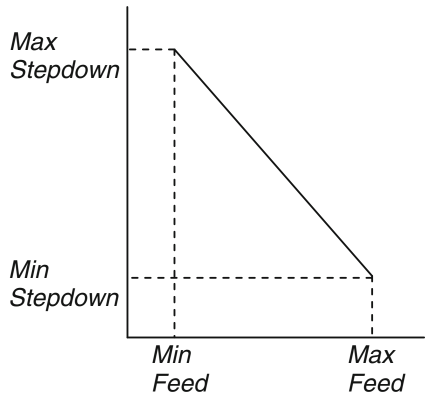


**Fig. 5** Stepdown–feed linear relation

Effects of Stepdown and feed rate on machining process efficiency are different in this model. As shown in Fig. 5, the ratio of feed rate increase is smaller than the ratio of Stepdown decrease because the feed rate increase is restricted by not only the cutter load, but also the dynamic characteristics of CNC machine motion system. Therefore, Stepdown is the primary parameter and has major effect on machining process efficiency, in this Stepdown–feed relation.

The length is another important property of milling cutters, because cutter length that is not long enough may cause collision between machine spindle and workpiece. In RPM system, machining zones are within the range of material deposition layer thickness, which is short relative to cutter length. Therefore, all cutters are assumed to have lengths larger than material deposition layer thickness; and cutter lengths are not included in the cutter library for machining process decision.

## 3 Finishing cutter selection algorithm

Finishing cutter selection algorithm framework is introduced first. Then, key technologies used in this algorithm (finishing cutter layer thickness, Stepdown calculation, AR calculation, and finishing cutter selection) are studied. The algorithm efficiency is also discussed in this section.

### 3.1 Finishing cutter selection algorithm framework

The finishing cutter selection algorithm flow chart is shown in Fig. 6. There are two major steps in this algorithm. In the beginning, finishing cutter layer thicknesses are decided according to the input STL model, and the calculated layer thickness data is stored in a finishing cutter layer thickness database *H*. Then finishing cutter geometry, cutter diameter, Stepdown, and feed rate for each finishing cutter layer are selected or calculated according to angle $\alpha$ of each finishing cutter layer. Sequence of the finishing cutter selection is from top layer to bottom layer because, for some layers, finishing cutter decision depends on the finishing cutter selection result of the layer above it.

### 3.2 Finishing cutter layer thickness

Finishing cutter layer thickness here is defined to be the effective range along $z$ axis of a specific finishing cutter. Angle $\alpha$ (surface slope angle) is identified as a key parameter for calculating finishing cutter layer thickness and Stepdown. And it is defined as the angle between a triangle facet and the horizontal plane.

In each triangle facet of the STL model, there is a normal vector $\vec{N}$ which is composed by $\vec{N}x$, $\vec{N}y$, and $\vec{N}z$ in 3-D coordinate system (Fig. 7a). From normal vector components $\vec{N}x$, $\vec{N}y$, and $\vec{N}z$, the angle between normal vector and horizontal plane is $\beta = arctg\left(Nz/\sqrt{Nx^2+Ny^2}\right)$. Relation between $\alpha$ and $\beta$ *is* $\alpha$=90°−$\beta$; therefore, the surface slope angle of the triangle facet is:

$$a = 90^\circ - arctg\left(Nz/\sqrt{Nx^2+Ny^2}\right) \tag{1}$$

By evaluating all triangles in a STL model, and selecting the smallest angle $\alpha$ at each $z$ position, a smallest angle $\alpha$ distribution along $z$ axis is obtained (see Fig. 7b). A continuous z position range which has the same smallest angle $\alpha$ is a finishing cutter layer; and this smallest angle $\alpha$ is the angle $\alpha$ of this finishing cutter layer.

In finishing cutter layer thickness calculation, tessellated facets with extremely tiny areas are neglected because tiny triangle facets are usually flaws of STL model, and triangle facets with tiny areas have little effect on geometry realization and cutter selection.

Output of finishing layer thickness calculation is a database *H* with structure illustrated in (2), where $h_1$, $h_2 \ldots$ $h_n$ are bottom and top $z$ heights of finishing cutter layers; and $\alpha_1$, $\alpha_2 \ldots \alpha_n$ are angle $\alpha$ of each layer.

$$\begin{array}{ll} [0, h_1] & a_1 \\ [h_1, h_2] & a_2 \\ [h_2, h_3] & a_3 \\ \ldots & \\ [h_{n-1}, h_n] & a_n \end{array} \tag{2}$$

### 3.3 Stepdown calculation

Finishing cutters could be flat-end cutters or sphere-end cutters. As shown in Fig. 8, when machining along a surface with angle $\alpha$ to the horizontal $x$–$y$ plane and with an allowable cusp height $L$, maximum Stepdown *SD* for both flat-end cutter and sphere-end cutter are calculated with formulas (3) and (4). Cusp height $L$ is the theoretical surface finish

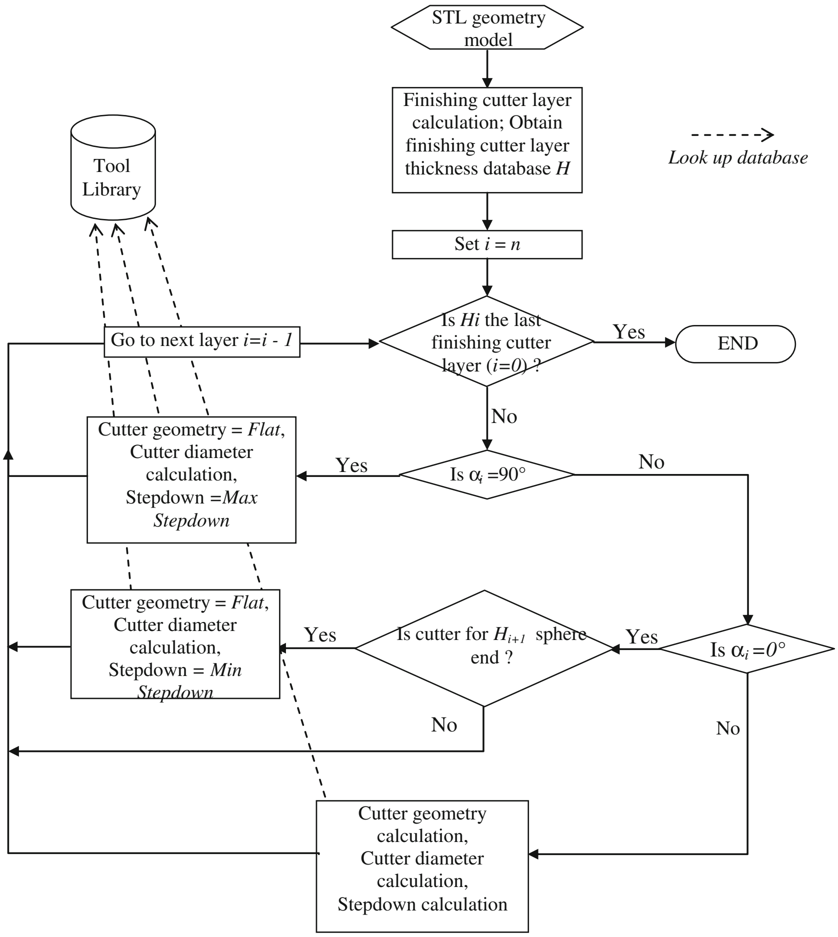


**Fig. 6** Finishing cutter selection algorithm flow chart

produced by successive cutter paths made by a cutter.

$$\mathrm{SD}_f = \frac{L}{\cos\alpha} \tag{3}$$

$$\mathrm{SD}_s = 2\sin\alpha\sqrt{2RL - L^2} \tag{4}$$

In these two situations, $X_f$ and $X_s$ are cutter center distance between two continuous tool paths, and can be calculated with formulas (5) and (6).

$$X_f = \frac{L}{\sin(\alpha)} = \mathrm{SD}_f ctg(\alpha) \tag{5}$$

$$X_s = 2\cos(\alpha)\sqrt{2RL - L^2} = SD_s ctg(\alpha) \tag{6}$$

When $L$ is fixed, $X_f$ and $X_s$ increase with the decreasing of angle $\alpha$. However, $X_f$ and $X_s$ cannot increase infinitely. When they are larger than $2R$ (cutter diameter), a gap appears

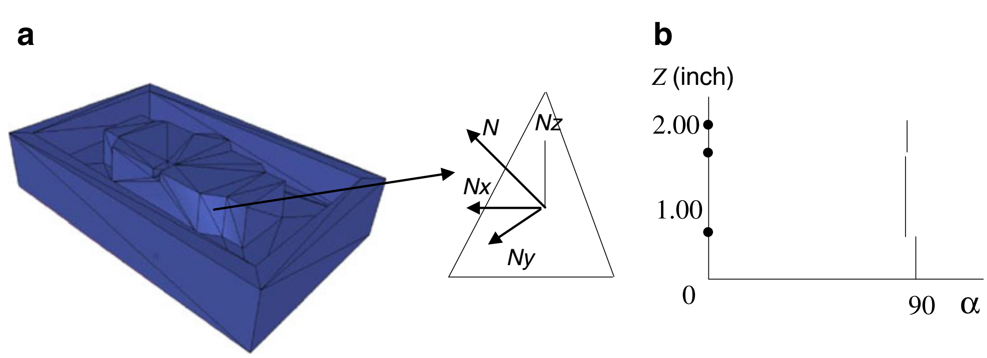


**Fig. 7** Surface slop angle calculation from STL model (**a**) and finishing cutter layers (**b**)

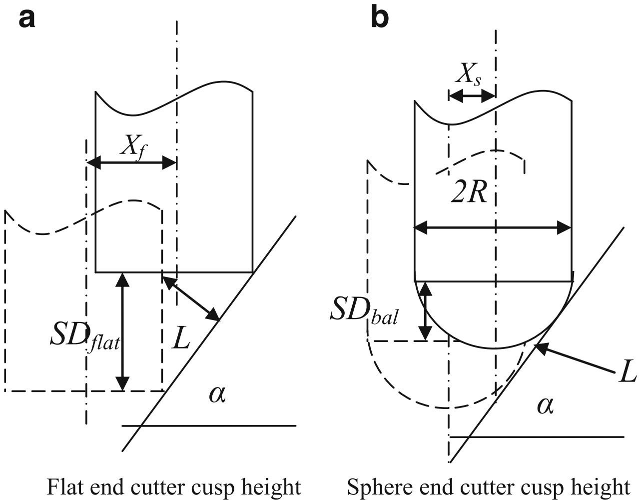


**Fig. 8** Flat-end cutter and sphere-end cutter cusp heights and Stepdowns; **a** flat-end cutter cusp height, **b** sphere-end cutter cusp height

between these two continuous tool paths. This gap is not allowed to happen. Therefore, Stepdown formulas are rewritten as:

$$\mathrm{SD}_f = \frac{L}{\cos\alpha} \quad (\text{when } L < 2R\sin(\alpha)) \\ = \frac{2R}{\mathrm{ctg}(\alpha)} \quad (\text{when } L > 2R\sin(\alpha)) \tag{7}$$

$$\mathrm{SD}_s = 2\sin\alpha\sqrt{2RL-L^2} \quad \left(\text{when } R > \cos(\alpha)\sqrt{2RL-L^2}\right) \\ = \frac{2R}{\mathrm{ctg}(\alpha)} \quad \left(\text{when } R < \cos(\alpha)\sqrt{2RL-L^2}\right) \tag{8}$$

## 3.4 Accessibility ratio calculation

AR is the percentage of a part surface that can be accessed by a specific cutter. It is an important index of machining quality; the finishing cutter diameter is selected per AR. In this work, AR is calculated by the polygonal geometry of a sliced STL model as follows.

$$\mathrm{AR} = \frac{\text{Length of accessible line segments}}{\text{Total length of line segments in the model}} \times 100\,\% \tag{9}$$

In formula (9), the total length of line segments in a slice of the sliced STL model or a layer of the model is represented by $L_{\mathrm{all}}$. In order to determine the length of accessible line segments, those inaccessible segments need to be detected and subtracted from $L_{\mathrm{all}}$. The inaccessible segments come from three situations, including undercuts, intersecting line segments, and concave corners. They are presented as follows.

### *3.4.1 Undercuts*

The first step is to evaluate the undercut accessibility. As illustrated in Fig. 9, an undercut situation is that a slice is totally covered by the union of slices above it. In this example, line segments of the undercut slice cannot be reached by cutters, because RPM system uses a three-axis vertical milling process. Whatever size the cutter is of, undercut line segments cannot be accessed; therefore, these undercut geometries are not included in AR calculation.

### *3.4.2 Intersecting line segments*

Finishing cutter paths are obtained by offsetting part geometry perimeters (sliced STL model) at each $z$ axis position by the finishing cutter radius. After offsetting, some line segments may intersect with one another, which implies that the distance between these features are small, and a cutter with this radius will result in an overcut in these areas. Therefore, these intersected line segments are inaccessible by cutters with the given radius. Length of these inaccessible line segments due to intersecting are represented by $L_{\mathrm{ins}}$.

Figure 10 shows the self-intersection and intersection between line segments on finishing cutter path. These line segments which cause intersection are inaccessible line segments. Part geometry contours after filtering inaccessible line segments are also shown in Fig. 10 (right side).

### *3.4.3 Concave corners*

As shown in Fig. 11, concave corners are partially or totally inaccessible. In this step, accessibility of line segments after (1) *undercut evaluation* and (2) *intersecting line segment calculation* are assessed by evaluating corner angles. If a corner angle is equal to or greater than 180° (convex corner), this corner is fully accessible by cutters with any diameter. However if the angle of corner is smaller than 180°, some

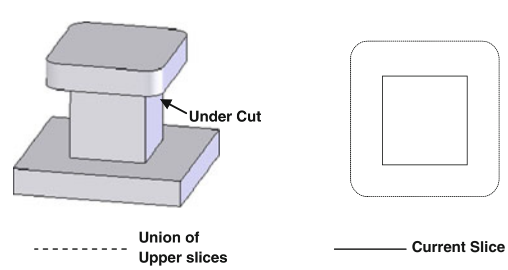


**Fig. 9** An undercut example

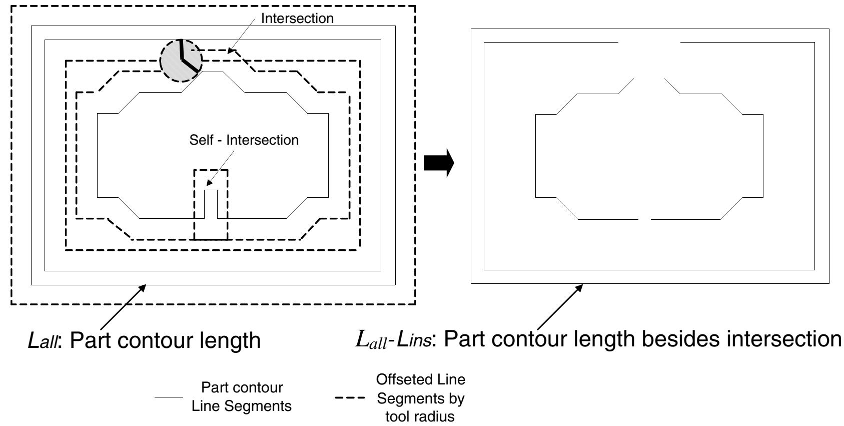


**Fig. 10** Intersecting line segments evaluation

sections of this corner are inaccessible. The length of inaccessible corner side line segments depends on the cutter diameter and corner angle. $L_{\mathrm{cor}}$ is inaccessible corner side line segment length calculated in this step. Figure 11 (right side) illustrates accessible line segments after filtering inaccessible corner side sections in a particular slice.

According to formula (9), AR of a specific cutter to the part geometry is calculated as:

$$\mathrm{AR} = \frac{L_{\mathrm{all}} - L_{\mathrm{ins}} - L_{\mathrm{cor}}}{L_{\mathrm{all}}} \times 100\% \tag{10}$$

Inaccessibility due to intersection is more important than the inaccessibility around concave corners in finishing cutter selection because inaccessibility due to intersection can be eliminated or reduced by selecting small cutters; on the contrary, inaccessibility around concave corners is inevitable. Therefore, a weight value $W$ is applied to balance the importance of these two types of inaccessible line segments. Then, the AR formula becomes:

$$\mathrm{AR} = \frac{L_{\mathrm{all}} - L_{\mathrm{ins}} \times W - L_{\mathrm{cor}}}{L_{\mathrm{all}}} \times 100\% \tag{11}$$

Sliced STL model uses line segments to approximate curves. This approximation imparts small errors on AR calculation. One method to reduce this error is to accommodate a certain degree of allowable deviation. A threshold AR can be decided by experience.

### 3.5 Finishing cutter selection

The cutter selection for each finishing cutter layer is divided into three situations, each of which is associated with a different angle $\alpha$.

#### *3.5.1 Layers with $\alpha$= 90°*

When angle $\alpha$ is 90°, finishing cutter machines the objective geometry with its shank. In this condition, flat-end cutters have better performance than sphere-end cutters, because flat-end cutters have uniform cylindrical surface from top to bottom, while sphere-end cutters have voids on the tip section.

Cutter diameter is decided with AR calculation. One characteristic of sand casting patterns is that the smallest cutter diameter is always required at the slice with $z = h_{i-1}$ for the finishing cutter layer $[h_{i-1}, h_i]$. Therefore, in the beginning of finishing cutter size selection for layer $[h_{i-1}, h_i]$, a sliced file at $z = h_{i-1}$ is obtained. Then, the allowable largest cutter diameter is determined according to AR calculated from the slice geometry at $z = h_{i-1}$.

The *Max Stepdown* of selected cutter is employed for Stepdown and feed rate calculation for optimal machining efficiency of this finishing cutter layer.

#### *3.5.2 Layers with $\alpha$= 0°*

A feature with 0° angle $\alpha$ is a plane. If the finishing cutter layer above it is machined with a sphere-end cutter, there will be material left by the sphere-end mill along plane edges. And a cleaning operation with a flat-end cutter is needed. Otherwise, no finishing operation is needed for 0° angle $\alpha$ planes.

The cutter diameter for flat plane edge cleaning is decided by AR calculation from the slice file obtained at the plane $z$ height. Flat plane feature is located at a specific $z$ axis height; therefore, there is no Stepdown for this operation. However, a Stepdown value is still needed for feed rate calculation. Because it is only a cleaning operation, which has minimum material to remove, *min Stepdown* of the selected cutter is adopted to maximize the feed rate, so that good machining efficiency is ensured.

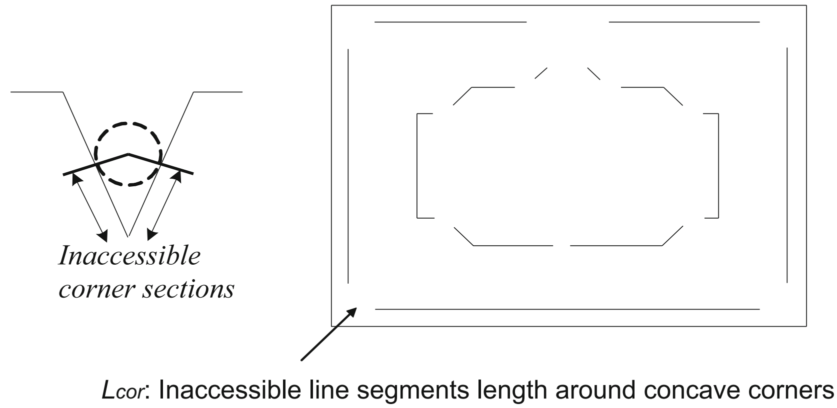


**Fig. 11** Concave corner accessibility assessment

*3.5.3 Layers with $0° < \alpha < 90°$*

In this condition, cutter geometry calculation needs to have cutter diameter as an input. Therefore, the cutter diameter decision with AR calculation is performed first. The same cutter diameter calculation procedure used in the angle $\alpha$=90° situation is employed.

When allowable cusp height $L$, angle $\alpha$, and cutter diameter $2R$ are known, both $SD_f$ and $SD_s$ are calculated with formulas (7) and (8). Considering from the perspective of process efficiency, if $SD_f > SD_s$, a flat-end cutter is adopted; otherwise a sphere-end cutter is employed. When $SD_f$ is equal to $SD_s$, a flat-end cutter is preferred. When cutter geometry is decided, the Stepdown is obtained at the same time. Then feed rate is calculated from the cutter Stepdown–feed relation.

3.6 Algorithm efficiency discussion

As stated in the beginning, good geometry realization (machining quality) is the primary goal when designing this algorithm; optimal algorithm efficiency is secondary. Some algorithm efficiency considerations have been discussed locally in previous sections. In this section, the overall algorithm efficiency is discussed.

Before applying this algorithm, a fixed cutter set strategy was employed in the RPM process. A sphere-end cutter with 0.25 in. diameter was used for finishing operation of every layer. This means that cavity features with smaller than 0.25 in. dimension in any direction cannot be fully created. In the meantime, both Stepdown and feed rate are fixed. In order to compromise different part geometries, a small Stepdown value (0.02 in.) had to be employed. Small Stepdown ensures small cusp heights when machining most of part geometries; however, it significantly hurts the process efficiency.

According to finishing cutter selection algorithm output, sphere-end cutters are selected in most times when angle $\alpha$ is between 0° and 90°, because they usually have better machining efficiency performance than flat-end cutters. Assuming the same 0.25 in. diameter sphere-end cutter is selected, finishing cutter selection algorithm output shows that the calculated Stepdown (with 0.002 in. cusp height) is smaller than 0.02 in. when angle $\alpha$ is smaller than 19°; it is between 0.02 and 0.06 in. when angle $\alpha$ is between 19° and 88°. When angle $\alpha$ is larger than 88°, the Stepdown is even much larger than 0.06 in. As discussed before, Stepdown has major impact on machining process efficiency in RPM process. Assuming angle $\alpha$ of objective geometries are evenly distributed between 0° and 90°, and 0.25 in. diameter sphere-end cutter is selected, more than 7/9 features will be machined with Stepdown larger than 0.02 in.. Therefore, process time by using finishing cutters selection algorithm is significantly shorter than that of using fixed cutter set strategy.

On the other hand, 0.25 in cutter diameter is relatively small for features in large sand casting patterns. However, the fixed cutter set strategy has to use a small cutter so that most of geometries can be successfully created. Finishing cutter selection algorithm selects cutters according to part geometries, which need larger than 0.25 in diameter cutters in most times. Large diameter cutters use large Stepdown

**Fig. 12** Additive/subtractive rapid pattern manufacturing machine at the Rapid Manufacturing and Prototyping Lab at Iowa State University

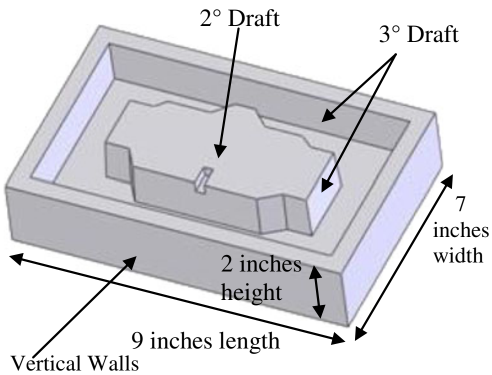


**Fig. 13** Sample pattern design

when the cusp height keeps the same. Therefore, this cutter diameter improvement from finishing cutter selection algorithm also significantly increases process efficiency. In summary, compared with the original fixed cutter set strategy, finishing cutter selection algorithm has significant improvement on finishing process efficiency.

## 4 Implementation

A RPM system has been developed and tested in the Rapid Manufacturing and Prototyping Laboratory at Iowa State University (Fig. 12). The system is comprised of four major functional elements including: (1) two elevator platforms serving as feed and build chambers with 1.2 $m^3$ (1,440 kg) capacities; (2) a material handling system to clamp, position, and compress up to 1.2 $m^2$ sheets of material; (3) a glue application system; and (4) one off-the-shelf component: a three-axis CNC router. A total of seven controllable axes are utilized in the completely automated processing of patterns. The gluing system utilizes a four-channel peristaltic pump which directs cyanoacrylate adhesive through a manifold applicator head. The servo-driven build table with four ball screw drives can position the pattern for cutting operations and apply up to 17,000 N of force during the 30-s gluing compression cycle. The finishing cutter selection algorithm has been implemented in software as a C-hook in the MasterCAM CAD/CAM environment. NC code for each layer and the requisite slab sequencing and facing to layer height data is output from MasterCAM and then processed using customized control system software to drive the machine elements.

The finishing cutter geometry, diameter, and Stepdown selection algorithm presented in this paper has been implemented in the RPM system; sample parts have been machined. In this section, results of a sample pattern machined with both the proposed algorithm and original fixed cutter set strategy are compared in aspects of machining quality and machining process time. By referring to "Pattern maker's manual" [31], cusp height $L$=0.002 in. is used in this pattern-making practice.

Sample pattern used in this study is shown in Fig. 13. This pattern has 9 in. length, 7 in. width, and 2 in. height. Outside walls of this pattern are vertical to horizontal plane, and inside surfaces have 2° or 3° drafts. There is also a small cavity on top, which requires small cutters to machine it out. MDF with dimensions of 10×8 in. and 0.75 in. thickness are the raw material for creating this sand casting pattern.

Finishing cutters in cutter library are listed in Table 1. There are eight finishing cutters in total: four flat-end cutters and four sphere-end cutters with diameter range from 1/8 to 1 in. The RPM machine spindle can rotate at up to 25,000 rpm. Cutter speeds and Stepdown–feed relations are selected according to cutter manufacturer's recommendation. When deciding cutter feed rates, machine structural rigidity and servo drive characteristics are also considered, besides considering cutter physical strengths. All cutters are made with high-speed steel material, which is good for machining wood fiber materials.

Finishing cutter layer thickness output and cutter selection results are listed in Table 2. Six layers in total are detected by finishing cutter selection algorithm (first column in Table 2). The finishing cutter selection process starts from the top layer as follows.

**Table 1** Finishing cutters in the cutter library

| Cutter diameter (inch) | Cutter geometry | Cutter speed (round/minute) | Stepdown–feed for MDF (inch, inch/min) | |
|---|---|---|---|---|
| 1 | Flat | 8,000 | (0.75, 125) | (0.01, 250) |
| | Sphere | 8,000 | (0.75, 125) | (0.01, 250) |
| 1/2 | Flat | 10,000 | (0.50, 100) | (0.01, 200) |
| | Sphere | 10,000 | (0.50, 100) | (0.01, 200) |
| 1/4 | Flat | 15,000 | (0.25, 75) | (0.005, 150) |
| | Sphere | 15,000 | (0.25, 75) | (0.005, 150) |
| 1/8 | Flat | 20,000 | (0.20, 50) | (0.005, 100) |
| | Sphere | 20,000 | (0.20, 50) | (0.005, 100) |

**Table 2** Finishing cutter selection algorithm output for the sample pattern

| Finishing cutter layers | Cutter geometry | Cutter diameter (inch) | Stepdown (inch) | Feed rate (inch/min) |
|---|---|---|---|---|
| [2.00, 2.00] 0° | N/A | N/A | N/A | N/A |
| [1.70, 2.00] 87° | Sphere | 0.125 | 0.044 | 90 |
| [1.70, 1.70] 0° | Flat | 0.125 | N/A | 100 |
| [0.75, 1.70] 87° | Sphere | 0.25 | 0. 063 | 132 |
| [0.75, 0.75] 0° | Flat | 0.25 | N/A | 150 |
| [0.00, 0.75] 90° | Flat | 1 | 0.75 | 125 |

To begin, the algorithm detects a flat plane feature on the pattern top. Because the deposited layer itself has a flat plane top, no finishing operation is needed for this layer.

For finishing cutter layer with $z$ axis height range from 1.70 to 2.0 in., it has outside vertical walls with 90° angle $\alpha$, inside walls with 87° angle $\alpha$, and the small cavity feature with 88° angle $\alpha$. Among these three angles, 87° is the smallest one. Therefore, the angle $\alpha$ for this layer is 87°. By AR calculation, the 0.125 in. cutter diameter is selected for finishing operation of this layer. And by comparing $SD_f$ and $SD_s$ of cutters with 0.125 in. diameter for surface with 87° angle $\alpha$, sphere-end cutter geometry is picked. Accordingly, $SD_s$ is 0.044 in. for this cutter; and feed rate is 90 in./min per calculation.

The next finishing cutter layer is a flat plane feature which has $z$ axis height at 1.70 in. Finishing cutter layer above it employed a sphere-end cutter; therefore, a single-pass finishing operation with a flat-end cutter is needed to clean edges. The AR calculation indicates that 0.125 in. cutter diameter is needed. No Stepdown is needed because there is only one $z$ axis height. And the fastest feed rate (100 in./min) for this cutter is adopted.

Finishing cutter layer with $z$ axis height range from 0.75 to 1.70 in. has 87° angle $\alpha$. The sphere-end cutter with 0.25 in. diameter is selected according to AR calculation and SD comparison. Stepdown is 0.063 in. according to calculation and feed rate is 132 in./min.

In the next layer, the flat plane at 0.75 $z$ axis height needs an edge cleaning operation too. Flat-end cutter with 0.25 in. diameter is selected. No Stepdown is needed and the feed rate is 150 in./min.

The bottom layer has $z$ axis position range from 0 to 0.75 in. It only has four vertical wall features with 90° angle $\alpha$. Because this finishing cutter layer has only outside boundaries, it always has 100 % AR for cutter with any diameter. Therefore, a flat-end cutter with largest diameter (1 in.) in the cutter library is selected. The largest Stepdown for this cutter (0.75 in.) is selected directly; the feed rate is 125 in./min. In this way, the outside wall finishing of this layer can be achieved in a single pass cutting with 1 in. diameter flat-end cutter.

This pattern was machined with both the fixed cutter set strategy and finishing cutter selection algorithm strategy. The traditional fixed cutter set strategy machined every layer with a 0.25 in. (diameter) sphere-end cutter for finishing; Stepdown and feed rate for this cutter are fixed at 0.02 in. and 125 in./min separately.

As shown in Fig. 14a, general machining quality of the fixed cutter set strategy is acceptable. However, the fixed cutter set strategy may miss some small features sometimes. In this case, the small slot feature on the top layer could not be machined out with the 0.25 in. diameter cutter (Fig. 14a), while the finishing cutter selection algorithm strategy presented in this paper successfully captured and machined this feature (Fig. 14b). The fixed cutter set strategy also used fixed Stepdown when machining each layer; therefore, the machining quality varies with part geometry. On the other

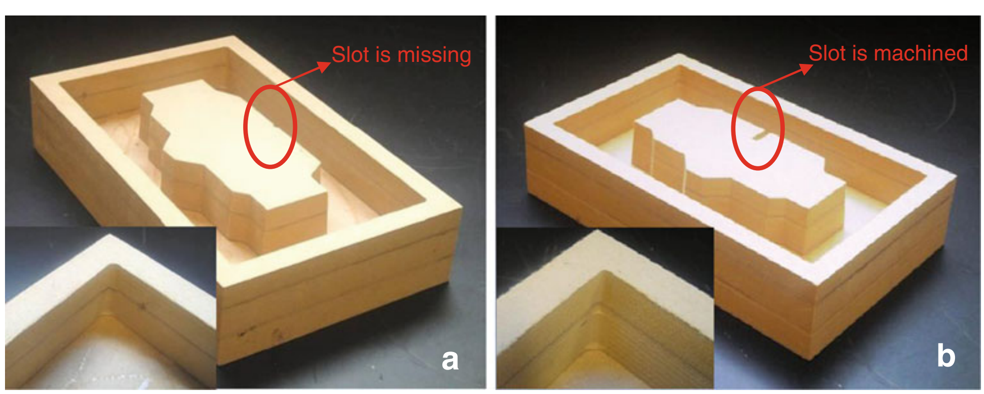


**Fig. 14** Machined sample patterns. **a** Pattern machined with fixed cutter set strategy, **b** pattern machined with finishing cutter selection algorithm strategy

hand, the finishing cutter selection algorithm strategy dynamically adjusted Stepdown according to part geometry; therefore, it ensures good machining quality.

Time consumed by the fixed cutter set strategy is much longer than that of finishing cutter selection algorithm strategy in this case: the finishing operation takes 59 min by using fixed cutter set strategy; and it only needs 20.4 min by employing the finishing cutter selection algorithm strategy. Time saving of this finishing cutter selection algorithm is significant when compared with fixed cutter set strategy.

## 5 Conclusion

Cutter geometry, cutter diameter, and machining parameters have significant impact on quality and efficiency in machining processes. This paper presented a finishing cutter selection algorithm for the RPM process, as the first part of cutter selection and optimization. Finishing cutter selection algorithm is able to improve machining quality and reduce machining time for RPM process. Even though high processing speed is not necessary for rapid prototyping and manufacturing techniques, slow fabrication speed inhibits the creation of large parts, such as sand casting patterns, with existing rapid prototyping and manufacturing methods. Therefore, the machining efficiency improvement for RPM process is meaningful.

The method presented in this paper effectively address the problem by analyzing three key aspects: finishing cutter geometry, cutter diameter, and Stepdown parameter. Finishing cutter layers are calculated from STL model first. Then finishing cutter geometry, diameter, and Stepdown are selected according to different angle $\alpha$ in each finishing cutter layer.

The algorithm has been implemented and tested. A sample pattern is machined with both fixed cutter set strategy and finishing cutter selection algorithm strategy. Experimental results show the proposed algorithm has significantly better performance with respect to both machining quality and efficiency over the existing fixed cutter set strategy. This finishing cutter selection algorithm is the first part of the whole cutter selection algorithm for RPM process. In the next part, the roughing cutter selection and semi-roughing cutter selection are going to be addressed with the purpose of both machining quality fulfillment and machining time saving.

## References


1. Luo XM, Frank MC (2010) A layer thickness algorithm for additive/subtractive rapid pattern manufacturing. Rapid Prototyping J 16(2):100–115
2. Frank MC, Wysk RA, Joshi SB (2004) Rapid planning for CNC milling—a new approach for rapid prototyping. J Manuf Syst 23(3):242–255
3. Ribeiro MV, Coppini NL (1999) An applied database system for the optimization of cutting conditions and cutter selection. J Mater Process Technol 92–93:371–374
4. Arezoo B, Ridgway K, Al-Ahmari AMA (2000) Selection of cutting cutters and conditions of machining operations using an expert system. Comp Ind 42(1):43–58
5. Lee YS, Chang TC (1994) Using virtual boundaries for the planning and machining of protrusion freeform features. Comput Ind 25(2):173–187
6. Lee YS, Chang TC (1995) Application of computational geometry in optimizing 2.5D and 3D NC surface machining. Comput Ind 26(1):41–59
7. Yao ZY, Gupta SK, Nau DS (2001) A geometric algorithm for finding the largest milling cutter. J Manuf Process 3(1):1–16
8. Bala M, Chang TC (1991) Automatic cutter selection and optimal cutter path generation for prismatic parts. Int J Prod Res 29(11):2163–2176
9. Chen YH, Lee YS, Fang SC (1998) Optimal cutter selection and machine plane determination for process planning and NC machining of complex surfaces. J Mach Syst 17(5):371–388
10. Arya S, Cheng SW, Mount DM (1998) Approximation algorithms for multiple cutter milling. Proceedings of the Fourteenth Annual Symposium on Computational Geometry, pp. 297–306
11. Veeramani D, Gau YS (1997) Selection of an optimal set of cutting-cutter sizes for 2½ D pocket machining. Comput Aided Des 29(12):869–877
12. Veeramani D, Gau YS (2000) Cutter-path generation using multiple cutting-cutter sizes for 2½ D pocket machining. IIE Trans 32(7):661–675
13. Nadjakova I, Mcmains S (2004) Finding an optimal set of cutter radii for 2D pocket machining. Proceedings of International Mechanical Engineering Congress and RD&D Expo, 1–8
14. Yao ZY, Gupta SK, Nau DS (2003) Algorithm for selecting cutters in multi-part milling problems. Comput Aided Des 35(9):825–839
15. Wang Y, Ma HJ, Gao CH, Xu HG, Zhou XH (2005) A computer aided cutter selection system for 3D die/mould-cavity NC machining using both a heuristic and analytical approach. Int J Comput Integr Manuf 18(8):686–701
16. D'Souza RM (2006) One setup level cutter selection for 2.5-D pocket milling. Robot Comput Integ Manuf 22(3):256–266
17. Lim T, Corney J, Clark DER (2000) Exact cutter sizing for feature accessibility. Int J Adv Manuf Technol 16(11):791–802
18. Lee YS, Choi BK, Chang TC (1992) Cut distribution and cutter selection for sculptured surface cavity machining. Int J Prod Res 30(6):1447–1470
19. Yang DCH, Han Z (1999) Interference detection and optimal cutter selection in 3-axis NC machining of free-form surfaces. Comput Aided Des 31(5):303–315
20. Lin AC, Gian R (1999) A multiple-cutter approach to rough machining of sculptured surfaces. Int J Adv Manuf Technol 15(6):387–398
21. Sun GP, Sequin CH, Wright PK (2001) Operation decomposition for freeform surface features in process planning. Comput Aided Des 33(9):621–636
22. Balasubramanima M, Joshi Y, Engels D, Sarma S, Shaikh Z (2001) Cutter selection in three-axis rough machining. Int J Prod Res 39(18):4215–4238
23. Joo J, Cho H, Yun W (1997) Efficient feature-based process planning for sculptured pocket machining. Comput Ind Eng 33(3–4):493–496
24. Perng DB, Cheng CT (1994) Feature based process plan generation from 3D DSG inputs. Comput Ind Eng 26(3):423–435

25. Chamberlain MA, Joneja A, Chang TC (1993) Protrusion features handling in design and manufacturing planning. Comput Aided Des 25(1):19–28
26. Chua MS, Rahman M, Wong YS, Loh HT (1993) Determination of optimal cutting conditions using design of experiments and optimization techniques. Int J Mach Cut Manuf 33(2):297–305
27. Yazar Z, Koch KF, Merrick T, Altan T (1994) Feed rate optimization based on cutting force calculations in 3-axis milling of dies and moulds with sculptures surfaces. Int J Mach Cut Manuf 34(3):365–377
28. Wang J, Armarego EJA (1995) Optimisation strategies and CAM software for multiple constraint face milling operations. Proceedings of the 6th International Conference on Manufacturing Engineering, 535–540
29. Rad MT, Bidhendi IM (1997) On the optimization of machining parameters for milling operations. Int J Mach Cut Manuf 37(1):1–16
30. Bae SH, Ko K, Kim BH, Choi BK (2003) Automatic feedrate adjustment for pocket machining. Comput Aided Des 35(5):495–500
31. AFS (1970) Pattern maker's manual. American Foundrymen's Society, Schaumburg, IL